SPECIAL ISSUE ARTICLE

EJN | European Journal of Neuroscience   FENS   WILEY

Low pre-stimulus EEG alpha power amplifies visual awareness but not visual sensitivity

Christopher S. Y. Benwell[1] | **Andra Coldea[2]** (iD) | **Monika Harvey[2]** | **Gregor Thut[2]**

[1]Division of Psychology, School of Social Sciences, University of Dundee, Dundee, UK

[2]Centre for Cognitive Neuroimaging, Institute of Neuroscience and Psychology, University of Glasgow, Glasgow, UK

Correspondence
Christopher S. Y. Benwell; School of Social Sciences, University of Dundee, Scrymgeour Building, Dundee DD1 4HN, UK.
Email: c.benwell@dundee.ac.uk

Gregor Thut, Institute of Neuroscience and Psychology, University of Glasgow, 62 Hillhead Street, Glasgow G12 8QB, UK.
Email: gregor.thut@glasgow.ac.uk

Associate Editor: Niko Busch

Abstract

Pre-stimulus oscillatory neural activity has been linked to the level of awareness of sensory stimuli. More specifically, the power of low-frequency oscillations (primarily in the alpha-band, i.e., 8–14 Hz) prior to stimulus onset is inversely related to measures of subjective performance in visual tasks, such as confidence and visual awareness. Intriguingly, the same EEG signature does not seem to influence objective measures of task performance (i.e., accuracy). We here examined whether this dissociation holds when stringent accuracy measures are used. Previous EEG-studies have employed 2-alternative forced choice (2-AFC) discrimination tasks to link pre-stimulus oscillatory activity to correct/incorrect responses as an index of accuracy/ objective performance at the single-trial level. However, 2-AFC tasks do not provide a good estimate of single-trial accuracy, as many of the responses classified as correct will be contaminated by guesses (with the chance correct response rate being 50%). Here instead, we employed a 19-AFC letter identification task to measure accuracy and the subjectively reported level of perceptual awareness on each trial. As the correct guess rate is negligible (~5%), this task provides a purer measure of accuracy. Our results replicate the inverse relationship between pre-stimulus alpha/ beta-band power and perceptual awareness ratings in the absence of a link to discrimination accuracy. Pre-stimulus oscillatory phase did not predict either subjective awareness or accuracy. Our results hence confirm a dissociation of the pre-stimulus EEG power–task performance link for subjective versus objective measures of performance, and further substantiate pre-stimulus alpha power as a neural predictor of visual awareness.

KEYWORDS

alpha, EEG, oscillations, perceptual awareness

Christopher S. Y. Benwell and Andra Coldea contributed equally to the manuscript.

---

1 | INTRODUCTION

Discovering the neural mechanisms underlying perception remains a fundamental challenge for neuroscience. A growing body of evidence suggests that neural oscillations in specific frequency bands, as measured on the scalp using electroencephalography (EEG), may play a functional role in various perceptual processes (Bonnefond et al., 2017; Fries, 2015; Gallotto et al., 2017; Keitel et al., 2018; Salinas & Sejnowski, 2001; Siegel et al., 2012; Thut et al., 2012; Varela et al., 2001). For instance, alpha-band (8–12 Hz) power prior to stimulus onset has consistently been shown to predict the likelihood of reporting the presence of a stimulus during detection tasks, with detection reports more likely in states of low alpha-power preceding stimulus onset (Busch et al., 2009; Chaumon & Busch, 2014; Ergenoglu et al., 2004; Iemi & Busch, 2018; Iemi et al., 2017; Kloosterman et al., 2019; Limbach & Corballis, 2016; Ruzzoli et al., 2019). In order to establish a theoretical underpinning of how fluctuations in alpha power relate to changes in perceptual performance, studies have recently started implementing psychophysical modelling techniques. One such formal framework comes from signal detection theory (SDT; Green & Swets, 1966; Macmillan & Creelman, 2005), whereby pre-stimulus alpha power could affect performance in the task by either (i) changing perceptual sensitivity to the target stimulus (i.e., the ability to detect/discriminate the veridical target) and/or by (ii) changing the decision criterion of the participant (or the internal representation of the target stimulus) and subsequently biasing responses. Iemi and colleagues (2017) proposed that if decreases in alpha power reflect an increase in global baseline excitability levels (see also evidence from transcranial magnetic stimulation [TMS]-EEG studies; Dugué et al., 2011; Romei et al., 2008; Samaha et al., 2017), then low alpha power may lead to a more liberal decision criterion, leaving perceptual sensitivity unaffected. In line with this view, a number of recent studies have shown that pre-stimulus alpha power influences the decision criterion and covaries with subjective measures of task performance (i.e., confidence and perceptual awareness) but not objective measures such as accuracy (Lange et al., 2013; Limbach & Corballis, 2016; Craddock et al., 2017; Iemi et al., 2017; Iemi & Busch, 2017; Samaha et al., 2017; Benwell et al., 2018; Kloosterman et al., 2019; Wöstmann et al., 2019; Samaha et al., 2020; see Samaha et al., 2020, for a review). Moreover, it has recently been shown that a more liberal decision criterion can be induced experimentally by using different stimulus-response reward contingencies, which results in a suppression of pre-stimulus alpha power (Kloosterman et al., 2019).

In line with these findings, we have recently shown that pre-stimulus EEG-power in the alpha/beta-bands over posterior sites inversely correlates with the level of subjective perceptual awareness of an upcoming threshold stimulus but does not predict objective performance (accuracy) when a decision has to be made regarding visual stimulus features (Benwell et al., 2017). Furthermore, we have found this relationship to be dependent on the stimulus being present and visible, consistent with a bias induced at the level of the perceptual experience rather than the decisional process per se (Chaumon & Busch, 2014; Iemi & Busch, 2017; Samaha, Iemi, et al., 2020). Here, we sought to replicate our previous findings (Benwell et al., 2017) in a larger sample of participants and using a different task, implemented to obtain a purer measure of objective task accuracy. In our previous experiment, we employed a 2-alternative forced choice (2-AFC) luminance discrimination task (Benwell et al., 2017). However, 2-AFC tasks have a 50% correct guess rate by chance, meaning that many 'correct' responses will be contaminated by guesses when typical peri-threshold stimuli are used. As a consequence, a trial-by-trial relationship between true performance accuracy and EEG measures may be more difficult to detect. Here, we employed a masked letter identification task using 19 different letters, in combination with single-trial ratings of perceptual awareness (Ramsøy & Overgaard, 2004). This 19-AFC task provides a purer measure of accuracy, because contamination by guesses is rendered negligible (~5% correct responses expected by chance). By introducing a purer measure of accuracy, we sought to implement a more rigorous test for a dissociation between objective and subjective aspects of visual task performance.

Based on our previous results, we hypothesized that pre-stimulus power would negatively predict subjective awareness ratings, but not discrimination accuracy. Additionally, we investigated the relationship between pre-stimulus oscillatory phase and perception, for which current evidence is mixed. Whilst many studies have linked the phase of oscillatory activity in specific frequency bands (before or during stimulus onset) to the likelihood of perception (Busch et al., 2009; Busch & VanRullen, 2010; Mathewson et al., 2009; Samaha et al., 2015), others have been unable to replicate these findings (Benwell et al., 2017; van Diepen et al., 2015; Ruzzoli et al., 2019; Vigué-Guix et al., 2020; see also Brüers & VanRullen, 2017). Together, our analyses aim to contribute to the understanding of the mechanisms by which baseline neural activity impacts visual perception.

2 | MATERIALS AND METHODS

2.1 | Participants

Twenty-two participants (17 females, mean age = 22.9 years, min = 18, max = 29) were recruited for the study. All reported normal or corrected-to-normal vision and no history of neurological or psychiatric disorders.

Each participant gave written informed consent and received monetary compensation for their participation in the study. The study was approved by the Ethics Committee of the College of Science and Engineering at the University of Glasgow. The experimental sessions were carried out within the Institute of Neuroscience and Psychology at the University of Glasgow.

2.2 | Task and experimental procedure

The task involved the identification of a briefly presented masked letter along with a subsequent rating of the level of awareness of the letter. The visual stimuli were presented on a CRT monitor (1,280 × 1,024 pixel resolution, 100-Hz refresh rate, viewing distance 57 cm) using E-Prime software (Version 2.0; Pittsburgh, Pennsylvania). Each trial (see Figure 1a) began with a white fixation cross presented on a grey background at the centre of the screen for a duration randomly varying between 2,500 and 3,000 ms. This was followed by presentation of a white target letter (subtending 2.2° visual angle) for one of five possible exposure durations (10, 20, 30, 40 or 50 ms).

The letter was randomly selected on each trial from a set of 19 consonants (BCDFGHJKLNPQRSTVXYZ). The letter was immediately followed by a patterned mask which consisted of all letters superimposed for 200 ms. After a delay period of 500 ms during which a blank screen was presented, participants were asked to indicate which letter they had perceived by pressing the corresponding letter key on a standard keyboard using their right index finger. Participants were instructed to guess if they had not perceived any letter. Immediately following the response, participants were asked to rate the clarity of their experience of the letter using the perceptual awareness scale (PAS; Ramsøy & Overgaard, 2004). The PAS scale consisted of the following categories: 1 – *no experience*, 2 – *brief glimpse*, 3 – *almost clear experience*, and 4 – *clear experience*. Responses were given by pressing one of four different buttons on the keyboard ('1', '2', '3' and '4' on the numeric pad). Each of the two response prompts stayed on the screen until the participants made a button press. The whole experiment consisted of 475 trials including 95 trials for each of the five presentation times (which were presented in a randomly intermixed order). A short break occurred every 95 trials. Participants completed a short block of practice trials prior to the main experiment to
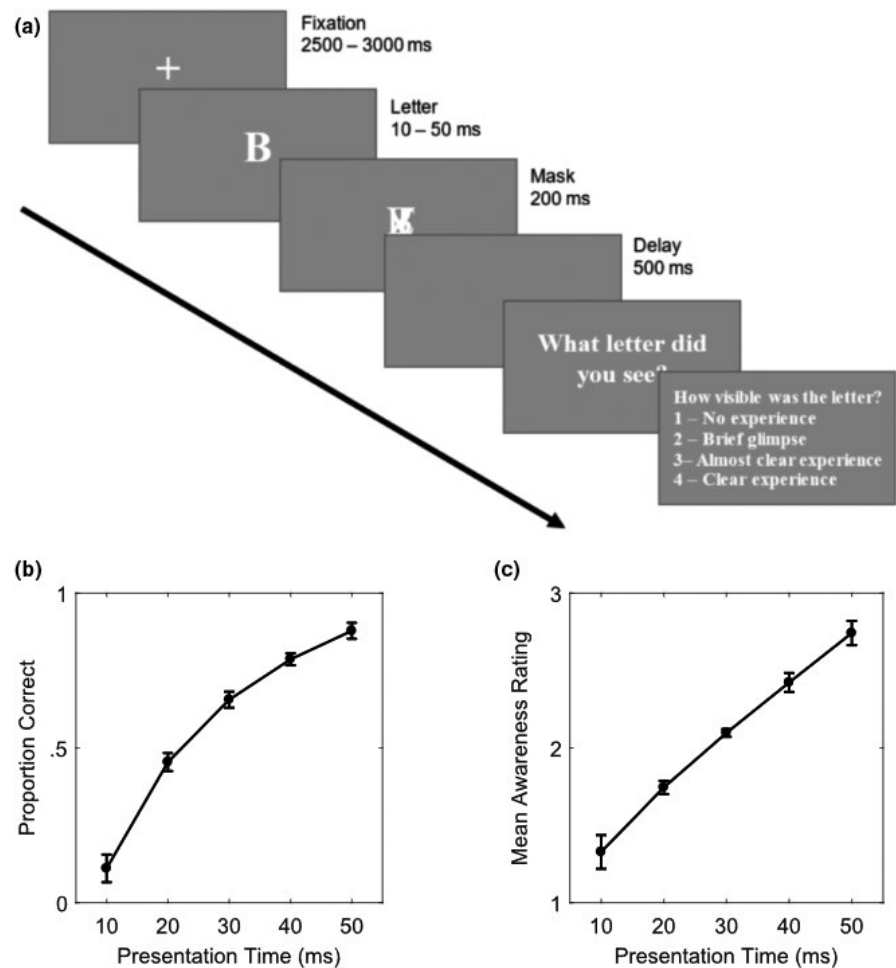

FIGURE 1 Task design and performance. (a) Each trial began with a white fixation cross presented for a jittered time between 2,500 and 3,000 ms, followed by the target stimulus—a consonant letter presented at 10, 20, 30, 40 or 50 ms, respectively. Immediately after, a mask appeared for 200 ms, followed by a blank screen for 500 ms. Then, a response prompt appeared, asking the participant which letter they saw. After the response, another prompt asked the participant to rate the quality of their perception on the four-point perceptual awareness scale. (b) Group-averaged proportion of correct responses as a function of presentation time. (c) Group-averaged mean awareness ratings as a function of presentation time. Both accuracy and awareness rating increased as a function of presentation time. All error bars indicate within-subject ± standard error (*SEM*)

familiarise themselves with the task. The entire experimental session lasted approximately 2 hr.

2.3 | Behavioural analysis

To evaluate the effectiveness of the experimental manipulation, statistical analyses were carried out separately for the proportion of correct responses and awareness ratings as the dependent variables and presentation time (10, 20, 30, 40 or 50 ms) as the independent variable. One-way repeated measures analyses of variance (ANOVA) were used. Additionally, effect-sizes were calculated using partial η^2 and Cohen's *d*.

2.4 | EEG recording

Continuous EEG was recorded with two BrainAmp MR Plus units (Brain Products GmbH, Munich, Germany) at a sampling rate of 1,000 Hz through 61 Ag/AgCl pellet pin scalp electrodes placed according to the 10–10 International System. Two extra electrodes served as ground (TP9) and online reference (AFz). Electrode impedances were kept below 10 kΩ. Preprocessing steps were performed using custom scripts incorporating EEGLAB (Delorme & Makeig, 2004) and FieldTrip (Oostenveld et al., 2011) functions in Matlab (Mathworks, USA).

Offline, continuous data were filtered for power line noise using a notch filter centred at 50 Hz. Additional low- (100 Hz) and high-pass (0.1 Hz) filters were applied using a zero-phase second-order Butterworth filter. The data were then divided into epochs spanning − 2.5:1.5 s relative to stimulus onset on each trial. Subsequently, excessively noisy electrodes were removed without interpolation, the data were re-referenced to the average reference (excluding ocular channels) and trials with abnormal activity were rejected using a semi-automated artefact detection procedure, in which trials with potential artefacts are identified based on (1) extreme amplitudes (threshold of ± 75 µV), (2) joint probability of the recorded activity across electrodes at each time point (probability threshold limit of 3.5 and 3 standard deviations [*SD*] for single-channel limit and global limit, respectively; pop_jointprob; Delorme & Makeig, 2004) and (3) kurtosis (local limit of 5 *SD*, global limit of 3 *SD*; pop_rejkurt; Delorme & Makeig, 2004). An average of 0.14 electrodes (min = 0, max = 2) and 12.8 trials (2.7%; min = 0, max = 68) was rejected across participants. An independent component analysis (ICA) was then run using the 'runica' EEGLAB function (Delorme & Makeig, 2004), and components corresponding to blinks, eye movements and muscle artefacts were removed.

Missing channels were then interpolated using a spherical spline method.

2.5 | Spectral analysis

Fourier-based spectro-temporal decomposition of the artefact-free single-trial data was performed using the 'ft_freqanalysis' function (wavelet convolution method: 'mtmconvol') from the FieldTrip toolbox (Oostenveld et al., 2011), yielding complex-valued time-frequency planes for each trial. A temporal resolution was maintained by decomposing overlapping 0.5-s segments of trial time series, consecutively shifted forward in time by 0.02 s. Data segments were multiplied with a Hanning taper and then zero-padded to a length of 1 s to achieve a frequency resolution of 1Hz across the range of 3:40 Hz. The data were then re-epoched from − 1 to 0.7 s relative to stimulus onset. We sought to investigate spectral EEG predictors of both discrimination accuracy and visual awareness ratings. The two spectral measures investigated were power and phase.

2.6 | EEG time-frequency power analysis

Single-trial power was obtained for all time-frequency points as follows:

$$EEG\,power\,(t,f) = |F(t,f)|^2,$$

where F is the complex Fourier coefficient corresponding to time window *t* and frequency *f*. The absolute power values across trials were then rank scored to mitigate the influence of outlying trials. PAS ratings and letter presentation times were also rank transformed for the EEG power analyses. To test for systematic relationships between pre-stimulus power and behavioural measures, data were analysed in the following steps:

Step 1: The *within-participant relationships* between single-trial power and both discrimination accuracy and visual awareness ratings were tested using separate models, in which EEG power and stimulus presentation time were entered as the predictors and the behavioural measure as the outcome variable. Stimulus presentation time was included as a predictor in the models in order to quantify the effect of EEG power independently of the effect of sensory evidence strength, and to test for any interaction between the two. For PAS ratings, coefficients were estimated for the following linear model:

$$Ratings = a + b_{EEG} * EEG + b_{PresTime} * PresTime + \varepsilon,$$

where *Ratings* represents the single-trial rank-transformed PAS ratings (1:4), *EEG* represents the single-trial rank-transformed power values, and *PresTime* represents the single-trial rank-transformed letter presentation times. The regression coefficient b_{EEG} indexes the direction and strength of the relationship between EEG power and PAS ratings that is independent of the relationship between letter presentation time and PAS ratings (indexed by $b_{PresTime}$). *a* is the model intercept and ε the error term. To test for an interaction between EEG power and letter presentation time, the following model was also run for each time electrode-time-frequency point:

$$Ratings = a + b_{int} * EEG * PresTime + \varepsilon,$$

where the regression coefficient b_{int} indexes the extent to which the effects of each predictor (EEG power and letter presentation time) on PAS Ratings are codependent. Both PAS Ratings models were implemented with the 'fitlm' function in Matlab R2020b (Mathworks, USA) using a least-squares solution.

For letter identification accuracy, a logistic regression was performed according to the following formula:

$$\log\left(\frac{P(Corr)}{1 - P(Corr)}\right) = a + b_{EEG} * EEG + b_{PresTime} * PresTime,$$

where b_{EEG} indexes the direction and strength of the relationship between single-trial EEG-power and the probability of being correct ($P(Corr)$) independently of the relationship between letter presentation time and accuracy (indexed by $b_{PresTime}$). To test for an interaction between EEG power and letter presentation time, the following model was also run for each time electrode-time-frequency point: $\log\left(\frac{P(Corr)}{1 - P(Corr)}\right) = a + b_{int} * EEG * PresTime$

where the regression coefficient b_{int} indexes the extent to which the effects of each predictor (EEG power and letter presentation time) on letter identification accuracy are codependent. Both accuracy models were implemented with the 'fitglm' function in Matlab R2020b (Mathworks, USA).

Step 2: For all four of the models described in Step 1, the regression coefficients were converted into *z* statistics relative to participant-specific null hypothesis distributions built by repeatedly shuffling (500 times) the mapping between the PAS ratings/letter identification accuracy and the predictors and recalculating the coefficients each time. This resulted in a z value for each participant, predictor and electrode-time-frequency point. We thus incorporated knowledge of the variability at the participant-level effects into the group-level analyses.

Step 3: At the *group level*, z scores were combined across participants for statistical analysis. More specifically, if at a given data point (electrode/frequency/time), EEG-power systematically covaries linearly with the perceptual measure (discrimination accuracy or awareness rating), then *z* scores should show a consistent directionality across participants. Alternatively, if there is no systematic linear relationship between EEG-power and the perceptual measure, then *z* scores across participants should be random (centred around 0). Hence, for each EEG/behaviour relationship, we performed two-tailed *t* tests (test against 0) on the *z*-score values across participants at all data points (i.e., all electrodes, frequencies and time points). Cluster-based permutation testing was employed in order to control the familywise error rate (FWER) across multiple comparisons (Maris & Oostenveld, 2007). Calculation of the test statistic involved the following: based on the initial *t* tests, all *t* values above a threshold corresponding to an uncorrected *p* value of 0.05 were formed into clusters by grouping together adjacent significant time-frequency points and electrodes. This step was performed separately for samples with positive and negative *t* values (two-tailed test). Note that for a significant sample to be included in a cluster, it was required to have at least 1 adjacent significant neighbouring sample. The spatial neighbourhood of each electrode was defined as all electrodes within approximately 5 cm, resulting in a mean of 6.3 (min = 3, max = 8) and median of seven neighbours per electrode. The *t* values within each cluster were then summed to produce a cluster-level *t* score (cluster statistic). Subsequently, this procedure was repeated across 2,000 permutations of the data (z scores from a random subset of participants were multiplied by − 1 and the two-tailed *t* test against 0 was calculated) with the largest cluster-level *t* score on each iteration being retained in order to build a data-driven null hypothesis distribution. The location of the original real cluster-level *t* scores within this null hypothesis distribution indicates how probable such an observation would be if the null hypothesis were true (no systematic difference from 0 in z scores across participants). Hence, if a given negative/positive cluster had a cluster-level *t* score lower than 2.5% or higher than 97.5% of the respective null distribution *t* scores, then this was considered a significant effect (5% alpha level).

2.7 | Bayes factor (BF) analysis of EEG time-frequency power results

In order to estimate evidence for both the null hypothesis (no relationship between EEG power and behavioural measure) and the alternative hypothesis (significant relationship between EEG power and behavioural measure), we also performed BF analyses. A BF below 1/3 indicates evidence for the null hypothesis, above 3 indicates evidence for the alternative hypothesis and between 1/3 and 3 indicates that the evidence is inconclusive (potentially due to a lack of statistical power). For all data points included in the significant

EEG power/behavioural measure clusters (detected in the regression analysis), the BF was calculated with a prior which followed a Cauchy distribution with a scale factor of 0.707 (Rouder et al., 2009). For each time point, the percentage of electrode-frequency points showing evidence for the null and alternative hypotheses respectively were calculated. This analysis was performed separately for both the awareness and accuracy data.

2.8 | Follow-up EEG power analysis

In our previous study, we found that the negative relationship between pre-stimulus power and awareness ratings scaled with the strength of the stimulus, being present for higher but not for the lowest stimulus intensities (nor for catch trials in which no stimulus was presented) (Benwell et al., 2017). In order to replicate this finding, we performed an additional analysis to test for this effect in the current experiment, using the data from electrode-time-frequency points included in any significant clusters prior to stimulus onset, and mirroring our previous analysis approach. Single-trial, cluster-averaged, pre-stimulus power values were extracted for each participant and trials were split into 'above' and 'below' median power bins. The proportion of correct responses and mean PAS ratings were then calculated separately for each presentation time (10, 20, 30, 40 and 50 ms) in each pre-stimulus power bin ('above' and 'below' median). Subsequently, repeated measures ANOVAs with the factors pre-stimulus cluster power (high, low) and presentation time were performed on both the accuracy and awareness rating measures separately.

2.9 | EEG time-frequency phase analysis

Step 1: To test for *within-participant relationships* between single-trial phase and both discrimination accuracy and visual awareness ratings, we employed a measure of circular-linear association called 'weighted intertrial phase clustering' (wITPC) (Cohen & Cavanagh, 2011; Cohen & Voytek, 2013). wITPC represents the resultant vector length (intertrial phase coherence) of single-trial phase angles, once the length of each individual vector has been weighted by the single-trial behavioural outcome (i.e., PAS rating or accuracy). Under the null hypothesis of no EEG phase-behaviour relationship, behavioural responses should be uniformly distributed across phase angles (and hence the average vector length would be close to zero). The magnitude of the average wITPC vector can be taken as a modulation of behaviour by phase angle.

wITPC was calculated for electrode-time-frequency point by multiplying the unit length complex-valued phase angle by the behavioural response on each trial, averaging those complex numbers across all trials, and taking the absolute value to obtain the average vector length. In order to quantify the effects of phase on behaviour independently of sensory evidence strength and for the PAS ratings and accuracy main effect analyses separately, we first retrieved the residual variations after regressing out the effect of letter presentation time on each behavioural measure. Hence, the wITPC was calculated here by multiplying the phase angle by the residual variation in behavioural responses, after regressing out the effect of letter presentation time, averaging those complex numbers across all trials and taking the absolute value to obtain the average vector length. PAS ratings, accuracy (coded 0 [incorrect] or 1 [correct]), regression residuals and letter presentation time were all rank transformed prior to calculation of the wITPC.

Step 2: Because the resulting magnitudes are not comparable across participants, and in order to control for possible nonuniformity of phase angles across trials (Cohen & Voytek, 2013), we applied within-participant permutation testing in which a participant-specific null hypothesis distribution was built by shuffling the observed phase and behavioural values with respect to one another across 500 iterations. The standardized distance between the actual wITPC value and the null distribution was taken as a *z* value corresponding to the probability of finding the observed behaviour-phase relationship by chance, given the observed data. The entire procedure was performed separately for the PAS ratings, accuracy and presentation time main effects, respectively.

Step 3: The group statistics on the single-participant wITPC *z* scores then proceeded exactly as described in Step 3 of the EEG power analysis above.

2.10 | BF analysis of EEG time-frequency phase results

As with the power analyses, we again calculated BFs to quantify the evidence for both the null hypothesis (no relationship between phase and behavioural measure) and the alternative hypothesis (significant relationship between phase and behavioural measure). Again, the BF was calculated for all data points included in the significant pre-stimulus EEG power/ PAS ratings cluster. For each time point, the percentage of electrode-frequency points showing evidence for the null and alternative hypotheses respectively was calculated separately for both the awareness and accuracy data.

2.11 | Phase opposition sum (POS) analysis

In order to replicate the method employed in our previous study (Benwell et al., 2017) and hence to allow the current

results to be directly comparable, we also employed a POS analysis (VanRullen, 2016a). This approach tested whether trials associated with one perceptual outcome (i.e., correct letter identification or high subjective awareness) differed in terms of their distribution of oscillatory phases for a given time-frequency point compared to trials associated with the opposite perceptual outcome (i.e., incorrect identification or low subjective awareness). POS analysis involves the comparison of inter-trial phase coherence (ITPC) measured over all trials (serving as a baseline) with ITPC measured separately for the trials from each condition (i.e., correct versus incorrect identification and high versus low subjective awareness). If the ITPC from each condition is larger than the total ITPC, then this suggests that the two perceptual outcomes are phase-locked to different phase angles.

ITPC was calculated as follows:

$$ITPC\ (t,f) = \left|\ \frac{1}{n} \sum_{k=1}^{n} \frac{F_k\ (t,f)}{|F_k\ (t,f)|}\ \right|,$$

where F is the complex Fourier coefficient corresponding to time window t and frequency f, n is the number of trials, and k is the individual trial index. The ITPC was calculated in this way over all trials and separately for those trials corresponding to correct identification, incorrect identification, high awareness ratings ('3' and '4' PAS ratings) and low awareness ratings ('1' and '2' PAS ratings), respectively.

Subsequently, the POS was calculated as follows:

$$POS = ITPC_A + ITPC_B - 2 * ITPC_{ALL},$$

where $ITPC_A$ and $ITPC_B$ are the ITPC calculated separately for the two trial types to be compared (i.e., correct versus incorrect response trials or high versus low awareness rating trials) and $ITPC_{ALL}$ is the ITPC calculated across all trials regardless of condition. POS will be positive when the ITPC of each trial group exceeds the overall ITPC; the main situation of interest, which indicates significant phase opposition between the two conditions.

Statistical analysis was first performed at the level of individual participants using a permutation test. For each participant, the trial assignment to Group A or B was randomly permuted 2,000 times and the POS value calculated and stored on each iteration. For each electrode-time-frequency point, the p value was calculated as the proportion of permutations that yielded a higher POS than the observed data. Hence, the p value reflects the likelihood of observing the actual POS value if the null hypothesis (no phase opposition) was true. The individual participant p-values were subsequently combined using Fisher's combined probability test (Fisher, 1925), which yielded a single group-level p value for each electrode-time-frequency point. In order to control for multiple comparisons, we employed nonparametric false discovery rate (FDR) correction (Benjamini & Yekutieli, 2001) across the pre-stimulus period with a threshold (q value) of 0.05.

Additionally, we equalized 'correct' and 'incorrect' trials (for the accuracy analysis) and 'high awareness rating' and 'low awareness rating' trials (for the awareness analysis) by randomly selecting from the higher likelihood outcome the same number of trials present for the lower likelihood outcome. This resulted in an average equalized number of trials per outcome across participants of 166 (min = 83, max = 233) for visual awareness ('high awareness rating' versus 'low awareness rating') and 170 (min = 106, max = 231) for accuracy ('correct' and 'incorrect'). This analysis was implemented because the POS loses statistical power when trial numbers are not equal between conditions (VanRullen, 2016a).

The wITPC and POS measures provide similar information about EEG phase-behaviour relationships. Whereas POS indexes whether there is a consistent difference in mean phase angle between binary behavioural outcomes (i.e., high versus low PAS ratings), the wITPC approach does not require a binary outcome measure (and hence no arbitrary binning of behavioural data) (Cohen & Cavanagh, 2011; Cohen & Voytek, 2013), and hence enabled a statistical approach that more closely approximates the EEG power—behaviour analyses, thereby facilitating comparison of the power and phase results.

2.12 | Pre-stimulus FFT analysis

Due to the temporal smearing inherent in time-frequency decomposition, which can lead to pre-stimulus EEG effects being contaminated by post-stimulus activity (Zoefel & Heil, 2013; van Diepen & Mazaheri, 2018; Brüers & VanRullen, 2017), we employed control analyses for both power and phase which included only pre-stimulus EEG time points ($-1:0$ s relative to stimulus onset) (see Samaha, Gosseries, et al., 2017 for a similar approach). Fast Fourier transforms (FFT) were performed on the clean, single-trial pre-stimulus waveforms at each electrode within each participant, using the 'mtmfft' method in FieldTrip (Maris & Oostenveld, 2007). The pre-stimulus data segments were windowed using a Hanning taper and zero-padded to a length of 1 s to achieve a frequency resolution of 1 Hz across the range of 3:40 Hz. The power- and phase-behaviour relationships were then tested using exactly the same three steps described above for the EEG-time-frequency analyses, but now with only the electrode and frequency dimensions: z statistics were calculated for both regression coefficients (power-behaviour analyses) and wITPC (phase-behaviour analyses) by permuting the mapping between EEG data and behaviour

500 times within each participant. The group statistics on the z scores proceeded exactly as described for the time-frequency analyses but with only two dimensions (electrodes and frequencies). Again, we calculated BFs to quantify the evidence for both the null and alternative hypotheses for each analysis. The BF was calculated for all electrode-frequency data points.

3 | RESULTS

3.1 | Behavioural results

The task involved the identification of one of 19 consonant letters that were displayed for 10–50 ms (five exposure durations) before being masked by a 200-ms letter compound stimulus (Figure 1a). Figure 1b plots the group-averaged proportion of correct responses as a function of presentation time, and Figure 1c plots the group-averaged awareness ratings. Both accuracy and awareness ratings increased as a function of presentation time. Mean proportions correct (Figure 1b) ranged from 0.1 ± 0.04 (10 ms) to 0.87 ± 0.02 (50 ms), whereby 0.053 represents chance-correct response rate (1/19 letters). Mean awareness ratings (Figure 1c) ranged from 1.3 ± 0.1 (10 ms) to 2.7 ± 0.07 (50 ms), hence from close to "no experience" (PAS 1) up to "almost clear experience" (PAS 3). The repeated measures ANOVA on the proportion of correct responses revealed a significant main effect of presentation time ($F[4, 84] = 314.595$, $p < .001$, $\eta_p^2 = 0.937$, linear contrast: $F[1, 21] = 992.168$, $p < .001$, $\eta_p^2 = 0.979$). Pairwise comparisons revealed significant increases in the proportion of correct responses across all presentation times (all p's < 0.001, min t value $= 5.893$, min Cohen's $d = 1.359$). The repeated measures ANOVA on the PAS ratings (subjective awareness) also revealed a significant main effect of presentation time ($F[4, 84] = 195.523$, $p < .001$, $\eta_p^2 = 0.903$, linear contrast: $F[1, 21] = 224.84$, $p < .001$, $\eta_p^2 = 0.915$). Pairwise comparisons revealed significant increases in PAS ratings across all presentation times (all p's < 0.001, min t value $= 9.679$, min Cohen's $d = 2.092$). Hence, the experimental manipulation of presentation time led to the expected increases in both identification accuracy and awareness ratings.

4 | EEG RESULTS

4.1 | Pre-stimulus power predicts visual awareness ratings but not discrimination accuracy

Figure 2a plots t values averaged across all electrodes at each time point (from -1 to $+0.7$ s post-stimulus) denoting the strength of the EEG power–PAS rating relationship, whilst controlling for the influence of stimulus strength (letter presentation time) on PAS ratings, across frequencies of 3–40 Hz. These t values represent group-level tests of whether regression coefficient (EEG power versus PAS rating) z scores from the individual single-trial analyses showed a systematic linear relationship across participants. We found one significant negative cluster (i.e., low power was associated with high PAS ratings and high power with low PAS ratings) which spanned across both pre- and post-stimulus time points (-0.84 to 0.7 s relative to stimulus onset, 3–31 Hz: cluster statistic $= -24,019$, $p = .0035$). For BFs from those electrode-frequency points included in the significant negative cluster, the percentage of data points providing evidence for H_1 far outnumbered those providing evidence for H_0 (see Figure 2a, bottom inset). In the pre-stimulus period of interest, the effect was widely distributed over almost all electrodes but with a right posterior maximum (see Figure 2b, left map: data averaged over all electrode-time-frequency points included in the cluster from -1 to 0 s relative to stimulus onset). Figure 2b (right map) shows the topographical representations of the post-stimulus portion of the negative cluster. Figure 2c (left panel) plots the group averaged frequency spectra computed separately for high PAS rating trials (red lines) and low PAS rating trials (black lines) from the data point corresponding to the peak t value in the pre-stimulus cluster (electrode POz, -0.54 s). Compared to low PAS rating trials, high PAS rating trials were associated with decreased pre-stimulus alpha power. This effect was highly consistent across participants as shown by the scatterplot (Figure 2c, right panel) of the difference in mean 10-Hz power between high and low PAS rating trials for each participant.

In contrast, no relationship was found between EEG power and identification accuracy, whilst controlling for the influence of stimulus strength on accuracy, during either the pre- or post-stimulus time periods (Figure 2d). For BFs from those electrode-frequency points included in the significant negative cluster from the awareness analysis, the percentage of data points providing evidence for H_0 far outnumbered those providing evidence for H_1, during the pre-stimulus period, though this pattern tended to reverse post-stimulus (see Figure 2d, bottom inset). Figure 2e (left panel) plots the group averaged frequency spectra computed separately for correct (red lines) and incorrect trials (black lines) from the data point corresponding to the peak t value in the visual awareness analysis (electrode POz, -0.54 s). No difference in power was observed between correct and incorrect trials (see also the scatterplot in Figure 2e [right panel] of the difference in mean 10-Hz power between correct and incorrect trials for each participant).

Both the PAS rating and accuracy results were confirmed when only pre-stimulus data (-1 to 0 s relative to stimulus onset) were included in the single-trial FFT analyses. Figure 3a plots t values averaged across all electrodes at each frequency (from 3 to 40) denoting the strength
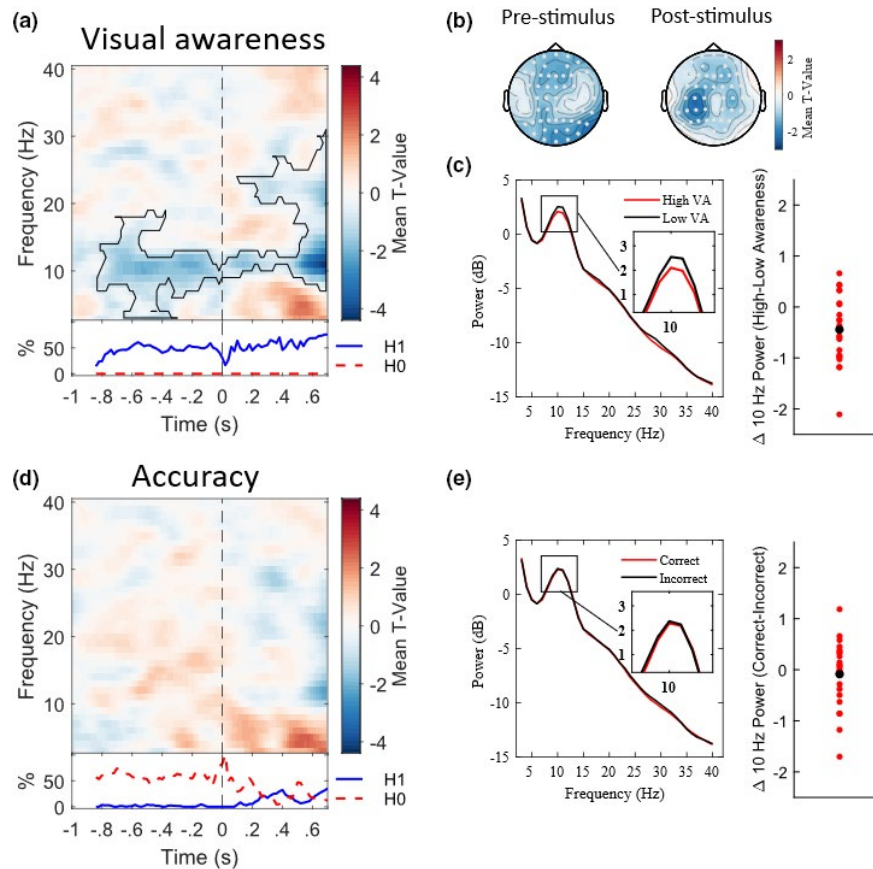
FIGURE 2 Relationship between oscillatory power and perception, controlling for letter presentation time. (a) The results of a single trial regression analysis revealed that pre-stimulus power was negatively correlated with visual awareness ratings (i.e., high power was associated with low PAS ratings and low power with high PAS ratings, black contour denotes significant cluster-corrected effects [$p < .05$]). Stimulus onset is highlighted by a vertical black dashed line. The bottom inset plots the time-course of the percentage of electrode-frequency points within the significant cluster with Bayes factors showing evidence for the null (H_0: no EEG/awareness relationship [dashed red line]) and alternative hypotheses respectively (H_1: significant EEG/awareness relationship [solid blue line]). As expected, the percentage of data points providing evidence for H_1 far outnumbered those providing evidence for H_0. (b) Plots the scalp topographies of the group-averaged effect separately for the pre- and post-stimulus portions of the significant negative cluster. In the pre-stimulus period of interest, the effect was widely distributed over almost all electrodes but with a posterior maximum (left map). Electrodes which were included in the significant cluster are highlighted in white. (c) Group-average frequency spectra computed separately for high PAS rating trials (red lines) and low PAS rating trials (black lines) in the pre-stimulus cluster. Compared to low PAS rating trials, high PAS rating trials were associated with decreased pre-stimulus alpha power. This effect was highly consistent across participants as shown by the scatterplot (right panel: black dot represents the mean difference value) of the difference in mean 10-Hz power between high and low PAS rating trials for each participant. (d) No relationship was found between EEG power and discrimination accuracy in any of the time-frequency ranges examined. The bottom inset plots the time-course of the percentage of electrode-frequency points from the significant pre-stimulus EEG/awareness cluster with Bayes factors showing evidence for the null (H_0: no EEG/accuracy relationship [dashed red line]) and alternative hypotheses respectively (H_1: significant EEG/accuracy relationship [solid blue line]). The percentage of data points providing evidence for H_0 far outnumbers those providing evidence for H_1 during the pre-stimulus period, though this pattern is reversed somewhat post-stimulus. (e) Group averaged frequency spectra computed separately for correct (red lines) and incorrect trials (black lines) within the pre-stimulus cluster that proved significant in the EEG/awareness analysis above. No difference in power was observed between correct and incorrect trials in this EEG/accuracy analysis. The right panel plots the difference in mean 10-Hz power between correct and incorrect trials for each participant (black dot represents the mean difference value)

and direction of the EEG power–PAS rating relationship, whilst controlling for the influence of stimulus strength on PAS ratings. One significant negative cluster was found which spanned from 9 to 12 Hz (cluster statistic = -103.4, $p = .0095$). In contrast, no significant relationship was found between EEG power and identification accuracy at any frequency (see Figure 3b).

4.2 | Follow-up EEG power analysis: no evidence that the pre-stimulus power-visual awareness relationship depends on stimulus strength

In order to test whether single-trial relationships between EEG power and the behavioural outcomes were dependent
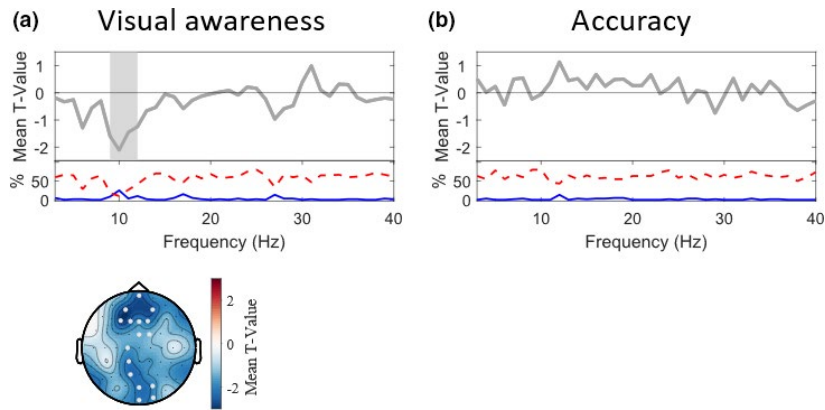
FIGURE 3 Single-trial fast Fourier transform analyses on pre-stimulus data confirm the relationship between pre-stimulus oscillatory power and perception. (a) Pre-stimulus power was negatively correlated with visual awareness ratings in the alpha (9–12 Hz) band (i.e., high power was associated with low PAS ratings and low power with high PAS ratings, grey background fill denotes significant cluster-corrected effects [$p < .05$]). The bottom inset plots the percentage of all electrodes with Bayes factors showing evidence for the null (H_0: no EEG/awareness relationship [dashed red line]) and alternative hypotheses respectively (H_1: significant EEG/awareness relationship [solid blue line]) across frequencies. The topographical representation of the effect is shown below the line plot. Electrodes which were included in the significant cluster are highlighted in white. (b) In contrast, no relationship was found between pre-stimulus power and discrimination accuracy in any frequency band

on the strength of the stimulus (letter presentation time), we performed additional interaction analyses. No significant interaction effects were found between EEG power and presentation time for either PAS ratings (Figure 4a) or identification accuracy (Figure 4b), when considering all electrode-time-frequency points or when considering only pre-stimulus time points in the FFT analysis (Figure 4c,d).

To directly replicate the analysis from our previous study (Benwell et al., 2017), we performed additional median power split repeated measures ANOVA analyses, using the single-trial data only from the pre-stimulus (−1:0 s) portion of the significant EEG power-PAS ratings cluster. The proportion of correct responses and mean PAS ratings were calculated separately for each presentation time in each power bin ('above' and 'below' median power) and participant. The corresponding group mean data are displayed for visual awareness ratings in Figure 4e and for proportion of correct responses in Figure 4f as a function of high (black dots/lines) and low power trials (red dots/lines) per presentation time.

The repeated measures ANOVA on the visual awareness ratings revealed a significant main effect of pre-stimulus power ($F[1, 21] = 9.946$, $p = .005$, $\eta_p^2 = 0.321$), a significant main effect of presentation time ($F[4, 84] = 196.274$, $p < .001$, $\eta_p^2 = 0.903$), but no significant pre-stimulus power × presentation time interaction ($F[4, 84] = 1.76$, $p = .145$, $\eta_p^2 = 0.077$). Hence, whilst we confirmed that pre-stimulus power relates to awareness ratings as in our previous study (Benwell et al., 2017), we found no significant evidence that the pre-stimulus EEG power–PAS ratings relationship was dependent on stimulus strength (in contrast to Benwell et al., 2017).

The repeated measures ANOVA on the proportion of correct responses revealed a significant main effect of presentation time ($F[4, 84] = 311.97$, $p < .001$, $\eta_p^2 = 0.937$) but no significant main effect of pre-stimulus power ($F[1,21] = 0.019$, $p = .892$, $\eta_p^2 < 0.001$) and no significant pre-stimulus power × presentation time interaction ($F[4, 84] = 1.772$, $p = .142$, $\eta_p^2 = 0.078$). Hence, there was also no evidence for an effect of pre-stimulus power on accuracy (or any interaction with letter presentation time), in line with the results of the regression analyses.

4.3 | No compelling evidence that pre-stimulus phase predicts visual awareness ratings or identification accuracy

Figure 5a plots t values averaged across all electrodes at each time point for the wITPCz analysis denoting the strength of the EEG phase–PAS rating relationship, whilst controlling for the influence of stimulus strength (letter presentation time) on PAS ratings, across frequencies of 3–40 Hz. The t values index group-level tests of whether weighting the single-trial phase vectors by their perceptual outcomes leads to an increase (positive values) or decrease (negative values) of the overall ITPC, relative to a participant specific null distribution. We found two significant positive clusters that were largely post-stimulus: a low frequency (3–13 Hz) cluster spanning − 0.14 to 0.7 s relative to stimulus onset (cluster statistic = 9,739.3, $p = .0025$), and a higher frequency (10–30 Hz) cluster spanning − 0.18 to 0.46 s relative to stimulus onset (cluster statistic = 5,363.4, $p = .01$). Figure 5b shows the topographical representations of the two clusters. Though
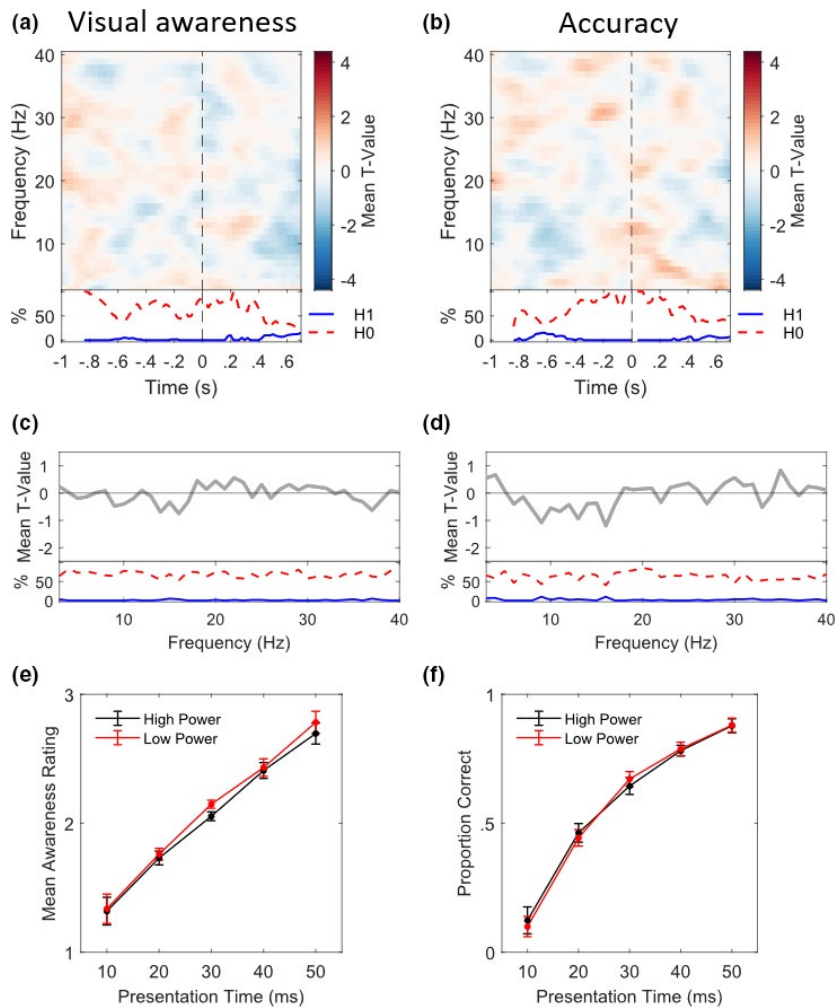
FIGURE 4 No interaction between oscillatory power and letter presentation time in predicting awareness ratings or accuracy. (a, b) The results of the single trial regression analysis revealed that the relationship between pre-stimulus power and visual awareness ratings (a) or accuracy (b) was not dependent on letter presentation time (interaction terms shown). Stimulus onset is highlighted by a vertical black dashed line. The bottom insets plot the time-course of the percentage of electrode-frequency points from the significant pre-stimulus EEG/awareness cluster (of Figure 2a) with Bayes factors showing evidence for the null (H_0: no EEG/presentation time interaction [dashed red line]) and alternative hypotheses respectively (H_1: significant EEG/presentation time interaction [solid blue line]). The percentage of data points providing evidence for H_0 far outnumbers those providing evidence for H1 during the pre-stimulus period. (C, D) Single-trial fast Fourier transform analyses restricted to pre-stimulus data confirmed the lack of interaction effects between pre-stimulus EEG power and letter presentation time when predicting either PAS ratings (c) or accuracy (d), respectively. The bottom insets plot the percentage of electrodes with Bayes factors showing evidence for the null (H_0: no EEG/presentation time interaction [dashed red line]) and alternative hypotheses respectively (H_1: significant EEG/presentation time interaction [solid blue line]) across frequencies. (e, f) Task performance after a median power split using single-trial data from the pre-stimulus portion of the significant EEG power–visual awareness cluster presented in Figure 2a. Group-averaged mean awareness ratings (e) and group-averaged proportion of correct responses (f) are shown as a function of presentation time for low (red lines) and high (black lines) power. Both accuracy and awareness rating increased as a function of presentation time in both power conditions, but no significant interaction between EEG power and presentation time was found for either PAS ratings or proportion correct. All error bars indicate within-subject $\pm$ standard error (*SEM*)

both clusters included time points immediately preceding and including stimulus onset, this likely reflects temporal smearing of primarily post-stimulus effects into the pre-stimulus period (Zoefel & Heil, 2013; van Diepen & Mazaheri, 2018; Brüers & VanRullen, 2017). Indeed, when only the pre-stimulus data (−1 to 0 s relative to stimulus onset) were included in the single-trial FFT analyses (thus ruling out any

contamination from post-stimulus activity), no significant relationship was found between EEG phase and PAS ratings at any frequency (see Figure 5c).

For the relationship between EEG phase and identification accuracy (Figure 5d), we found one significant positive cluster that was largely post-stimulus (−0.06:0.7 s relative to stimulus onset, 3:24 Hz: cluster statistic = 19,079, $p < .001$)
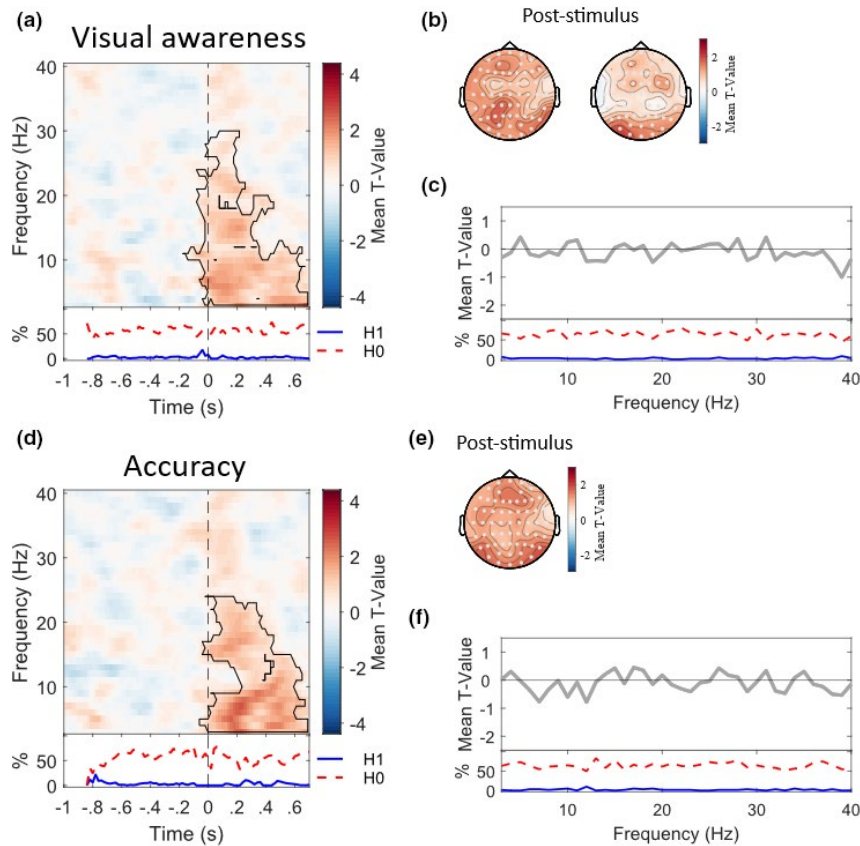
FIGURE 5 Relationship between oscillatory phase and perception, controlling for letter presentation time. (a) Time-frequency map of single trial phase modulations by visual awareness rating residuals (with the effect of letter presentation time on awareness ratings regressed out) from a weighted ITPC z score (wITPCz) analysis. These t-values index group-level tests of whether weighting the single-trial phase vectors by their perceptual outcomes leads to an increase (positive values) or decrease (negative values) of the overall ITPC, relative to a participant specific null distribution. Black contour denotes significant cluster-corrected effects ($p < .05$, significant clusters collapsed together). Stimulus onset is highlighted by a vertical black dashed line. The bottom inset plots the time-course of the percentage of electrode-time-frequency points from the significant pre-stimulus EEG power/awareness cluster with Bayes factors showing evidence for the null (H_0: no EEG phase/awareness relationship [dashed red line]) and alternative hypotheses respectively (H_1: significant EEG phase/awareness relationship [solid blue line]). (b) Plots the scalp topographies of the group-averaged effects separately for the two significant positive clusters. Electrodes which were included in the significant cluster are highlighted in white. (c) No relationship was found between pre-stimulus phase and awareness ratings when only pre-stimulus data (-1–0 s relative to stimulus onset) were included in the single-trial fast Fourier transform (FFT) analysis (thus ruling out any contamination from post-stimulus activity). The bottom inset plots the percentage of electrodes with Bayes factors showing evidence for the null (H_0: no EEG phase/ awareness relationship [dashed red line]) and alternative hypotheses respectively (H_1: significant EEG phase/awareness relationship [solid blue line]). (d) Time-frequency map of single trial phase modulations by accuracy. These t values index the group-level strength and direction of the phase locking–accuracy relationship. The bottom inset plots the time-course of the percentage of electrode-time-frequency points from the significant pre-stimulus EEG power/awareness cluster with Bayes factors showing evidence for the null (H_0: no EEG phase/accuracy relationship [dashed red line]) and alternative hypotheses respectively (H_1: significant EEG phase/accuracy relationship [solid blue line]). (e) Plots the group-averaged scalp topography of the significant positive cluster. (f) Again, no relationship was found between pre-stimulus phase and accuracy when only pre-stimulus data were included in the single-trial FFT analysis

(see map in Figure 5e for a topographic representation of the cluster). Again, when only pre-stimulus data were included in the single-trial FFT analyses, no significant relationship was found between EEG phase and accuracy at any frequency (see Figure 5f).

Similar relationships were observed between EEG phase and both PAS ratings and identification accuracy in two variants of the above analyses, with all relationships confined to the post-stimulus window (reported as Supplementary

Material). First, when letter presentation time was not controlled for, additional significant negative clusters were observed at early post-stimulus time points across low frequencies (see Figure S1a,b,d,e). These negative clusters hence likely reflect the covariation of letter presentation time with post-stimulus phase locking. Indeed, an additional analysis of the phase-presentation time main effect showed significant effects which largely overlapped in time, space and frequency (see Figure S1g,h). Furthermore, no significant

phase effects were observed for any of the single-trial FFT analyses when only pre-stimulus EEG data were included (Figure S1c,f). Second, a POS analyses (replicating Benwell et al., 2017) also provided no evidence for a relationship between pre-stimulus phase and either PAS ratings or identification accuracy (see Figure S2).

Overall, the data indicate that the significant EEG phase–behaviour relationships we observed originated entirely in stimulus-evoked neural activity (Brüers & VanRullen, 2017; Del Cul et al., 2007; van Diepen & Mazaheri, 2018; Tagliabue et al., 2019), and so we find no compelling evidence for an influence of spontaneous pre-stimulus oscillatory phase on perception in our data set.

5 | DISCUSSION

In this study, we implemented a letter discrimination task to examine the effects of pre-stimulus oscillatory activity on both discrimination accuracy and perceptual awareness ratings. Single-trial regression analyses revealed a negative correlation between pre-stimulus power (~9–12 Hz, Figure 3) and subjective awareness ratings, but no relationship between pre-stimulus power and discrimination accuracy. In contrast, we did not find strong evidence that pre-stimulus oscillatory phase predicted subjective awareness ratings nor accuracy in any frequency band. These results largely replicate those reported by Benwell and colleagues (2017), but this time using an mAFC paradigm rather than a 2-AFC paradigm. Taken together, these experiments emphasize a dissociation between pre-stimulus neural predictors of subjective and objective measures of task performance and shed light on the processes by which pre-stimulus oscillatory activity influences visual perception.

Several recent studies employing formal psychophysical models (e.g., SDT; Green & Swets, 1966) have contributed to a better understanding of the relationship between baseline neural activity and visual perception. These studies have found correlations between pre-stimulus alpha suppression and a liberal decision criterion (Iemi et al., 2017; Limbach & Corballis, 2016). Furthermore, observers can exert deliberate control over fluctuations in pre-stimulus alpha activity when a more liberal decision criterion is experimentally induced (Kloosterman et al., 2019). Hence, baseline alpha activity seems to relate to bias in perceptual reports rather than perceptual sensitivity, possibly because it reflects changes in global baseline excitability (Romei et al., 2008) that may affect both signal and noise (Iemi et al., 2017). This account is represented by the baseline sensory excitability model (BSEM) proposed by Samaha, Iemi, et al., (2020).

One question is then at what stage posterior baseline alpha activity/excitability interacts with information processing during perceptual tasks. In order to bias reports, increased

baseline excitability could modulate the observers' decision-making strategy (i.e., induce a decision bias) and/or amplify their subjective perception (i.e., induce a perceptual bias) (Iemi et al., 2017; Samaha, Iemi, et al., 2020). Recently, Iemi and Busch (2018) have provided compelling evidence that pre-stimulus alpha power induces changes in perceptual experience, rather than the decision criterion alone, in an experiment involving a two-interval forced choice (2IFC) task. Another line of research providing evidence that baseline alpha-power biases subjective perceptual experience comes from studies measuring subjective reports of performance. In 2-AFC discrimination tasks, pre-stimulus power is negatively correlated with perceptual awareness/subjective visibility ratings (Benwell et al., 2017; Samaha, LaRocque, et al., 2020) and decision confidence (Samaha, Iemi, et al., 2017; Wöstmann et al., 2019), but there is no effect of pre-stimulus power on accuracy, neither in visual nor auditory modalities. A similar dissociation has been reported for pre-stimulus alpha-power and idiosyncratic biases versus accuracy (Grabot & Kayser, 2020). In addition, Benwell et al., (2017) found the negative correlation between pre-stimulus alpha power and awareness to be contingent on the stimulus being present (no such correlation in catch trials) and to depend on stimulus-intensity (see also Chaumon & Busch, 2014). This was taken as further evidence for the pre-stimulus alpha-perception link reflecting a perceptual rather than decisional bias. In the current experiment, we did not implement catch trials, as there was no stimulus-absent condition, and we were unable to fully replicate the aforementioned dependency of the alpha-perception relationship on stimulus-intensity (i.e., stimulus presentation times). However, a similar pattern as in Benwell et al., (2017) was observed (i.e., stronger influence of pre-stimulus alpha on awareness ratings at longer presentation times; see Figure 4e: 30 and 50 ms versus 10, 20 and 40 ms presentation times), although the relationship between pre-stimulus alpha power and awareness ratings did not significantly differ across letter presentation times. Overall, we therefore believe that the current results remain mostly in line with a model positing that baseline alpha activity/excitability modulates perceptual experience directly rather than only modulating decision bias.

Mechanistically, changes in subjective perceptual experience as a function of alpha-band modulations may result from an effect on early sensory responses (Samaha, Iemi, et al., 2020), a response gain mechanism at late perceptual stages (e.g., Benwell et al., 2017; Chaumon & Busch, 2014), or through a combination of both (see Iemi et al., 2019). The evidence for either an early or a late perceptual account is inconclusive so far, and the present data cannot speak directly to this issue. More direct tests of the stage at which baseline alpha activity interacts with stimulus processing may be obtained from the analysis of visual evoked potentials and their comodulation with pre-stimulus alpha activity. Gundlach and

colleagues (2020) measured ongoing alpha-band oscillations and steady-state visual evoked potentials (SSVEPs) simultaneously, to establish whether alpha-band modulations relate to early sensory input gain. Using a spatial cueing paradigm, they showed that the amplitudes of both SSVEPs and alpha-band oscillations are modulated by spatial attention but that their modulations vary independently of each other and have different temporal dynamics (Gundlach et al., 2020; see also Keitel et al., 2019 and Antonov et al., 2020). This is supportive of a role of alpha-band oscillations beyond early sensory processing. In line with these findings, Zhigalov and Jensen (2020) implemented a novel broadband frequency tagging technique and found that the sources of alpha oscillations were localized around the parieto-occipital sulcus, rather than the primary visual cortex. By contrast, Iemi et al., (2019) found an early component of the visual evoked potential (C1) to comodulate with spontaneous pre-stimulus alpha power, suggesting that alpha may have an inhibitory effect on early stages of sensory processing (see also Zazio et al., 2020). The source of these discrepancies in the literature is unclear. Further research is needed to disentangle the influence of pre-stimulus EEG power on different post-stimulus processing stages.

In addition to alpha power, the phase of low frequency rhythms has been suggested to play an important role in visual perception (Mathewson et al., 2011; VanRullen, 2016b), although the evidence appears more mixed for the pre-stimulus phase- than the pre-stimulus power-perception link. The phase of pre-stimulus oscillations in the alpha-band has been associated with both the detection probability of near-threshold stimuli as well as discrimination accuracy between two rapidly presented visual stimuli (Busch et al., 2009; Mathewson et al., 2009; Milton & Pleydell-Pearce, 2016; Ronconi et al., 2017; Samaha et al., 2015). However, a recent registered report by Ruzzoli et al., (2019) failed to replicate the seminal finding that spontaneous pre-stimulus alpha-phase correlates with visual target detection. In the present experiment, we found no compelling evidence that pre-stimulus oscillatory phase predicts either subjective awareness or accuracy in a letter identification task, replicating the results of Benwell et al. (2017). When only pre-stimulus EEG data were included in the single-trial analyses (thus ruling out any contamination from post-stimulus activity), no significant relationship was found between phase and either awareness ratings or accuracy at any frequency. The discrepancy with previous findings may be due to differences in experimental design. We presented the stimuli at varying time intervals from trial onset, which might have precluded phase from influencing perception. Samaha and colleagues (2015) found more phase consistency when participants expected the visual target onset, compared to when the visual stimuli were unexpected, whilst others have argued against a top-down modulation of alpha-phase even when the targets were temporally predictable (van Diepen et al., 2015). Additionally, in the present study, the visual stimuli were visible such that on average, identification accuracy was above threshold, whilst many previous studies reported a phase effect on perception when stimuli were near-threshold (see Busch et al., 2009; Mathewson et al., 2009). However, discrepancies found in the literature could also be due to contamination of the signal by target-locked, post-stimulus phase differences and temporal distortions of these phase effect towards pre-stimulus latencies (Brüers & VanRullen, 2017), a scenario that likely explains the pattern of results observed in the time-frequency wITPCz analyses here. Overall, our results add to a growing body of studies casting doubt on the effect of pre-stimulus phase on visual perception (Benwell et al., 2017; van Diepen et al., 2015; Ruzzoli et al., 2019; Vigué-Guix et al., 2020).

In conclusion, the present findings substantiate a growing body of evidence linking pre-stimulus EEG alpha power to subjective rather than objective psychophysical measures. Hence, pre-stimulus alpha power represents a neural predictor of the level of perceptual awareness, which is dissociated from perceptual sensitivity.

CONFLICT OF INTEREST
The authors declare no competing financial interests.

AUTHOR CONTRIBUTIONS
C.S.Y.B., A.C., M.H. and G.T. designed research; C.S.Y.B. and A.C. performed research; C.S.Y.B., A.C. and G.T. analysed data; C.S.Y.B., A.C., M.H. and G.T. wrote the paper.

PEER REVIEW
The peer review history for this article is available at https://publons.com/publon/10.1111/ejn.15166.

DATA AVAILABILITY STATEMENT
Raw data and codes are available upon request to the corresponding authors.

ORCID
Andra Coldea https://orcid.org/0000-0002-8010-4541

REFERENCES
Antonov, P. A., Chakravarthi, R., & Andersen, S. K. (2020). Too little, too late, and in the wrong place: Alpha band activity does not reflect an active mechanism of selective attention. *NeuroImage*, *219*, 117006. https://doi.org/10.1016/j.neuroimage.2020.117006

Benjamini, Y., & Yekutieli, D. (2001). The control of the false discovery rate in multiple testing under dependency. *Annals of Statistics*, *29*, 1165–1188.

Benwell, C. S. Y., Keitel, C., Harvey, M., Gross, J., & Thut, G. (2018). Trial-by-trial co-variation of pre-stimulus EEG alpha power and visuospatial bias reflects a mixture of stochastic and deterministic effects. *European Journal of Neuroscience*, *48*, 2566–2584.

Benwell, C. S. Y., Tagliabue, C. F., Veniero, D., Cecere, R., Savazzi, S., & Thut, G. (2017). Prestimulus EEG power predicts conscious awareness but not objective visual performance. *Eneuro*, *4*, ENEURO.0182-17.2017. https://doi.org/10.1523/ENEURO.0182-17.2017

Bonnefond, M., Kastner, S., & Jensen, O. (2017). Communication between brain areas based on nested oscillations. *Eneuro*, *4*, ENEURO.0153-16.2017. https://doi.org/10.1523/ENEURO.0153-16.2017

Brüers, S., & VanRullen, R. (2017). At what latency does the phase of brain oscillations influence perception? *Eneuro*, *4*, ENEURO.0078-17.2017.

Busch, N. A., Dubois, J., & VanRullen, R. (2009). The phase of on-going EEG oscillations predicts visual perception. *Journal of Neuroscience*, *29*, 7869–7876. https://doi.org/10.1523/JNEUROSCI.0113-09.2009

Busch, N. A., & VanRullen, R. (2010). Spontaneous EEG oscillations reveal periodic sampling of visual attention. *PNAS*, *107*, 16048–16053. https://doi.org/10.1073/pnas.1004801107

Chaumon, M., & Busch, N. A. (2014). Prestimulus neural oscillations inhibit visual perception via modulation of response gain. *Journal of Cognitive Neuroscience*, *26*, 2514–2529. https://doi.org/10.1162/jocn_a_00653

Cohen, M. X., & Cavanagh, J. F. (2011). Single-trial regression elucidates the role of prefrontal theta oscillations in response conflict. *Frontiers in Psychology*, *2*, 30.

Cohen, M. X., & Voytek, B. (2013). Linking nonlinear neural dynamics to single-trial human behavior. In M. (Meyer) Z. Pesenson (Ed.), *Multiscale analysis and nonlinear dynamics* (pp. 217–232).

Craddock, M., Poliakoff, E., El-deredy, W., Klepousniotou, E., & Lloyd, D. M. (2017). Pre-stimulus alpha oscillations over somatosensory cortex predict tactile misperceptions. *Neuropsychologia*, *96*, 9–18. https://doi.org/10.1016/j.neuropsychologia.2016.12.030

Del Cul, A., Baillet, S., & Dehaene, S. (2007). Brain dynamics underlying the nonlinear threshold for access to consciousness. *PLoS Biology*, *5*, e260.

Delorme, A., & Makeig, S. (2004). EEGLAB: An open source toolbox for analysis of single-trial EEG dynamics including independent component analysis. *Journal of Neuroscience Methods*, *134*, 9–21. https://doi.org/10.1016/j.jneumeth.2003.10.009

Dugué, L., Marque, P., & VanRullen, R. (2011). The Phase of Ongoing Oscillations Mediates the Causal Relation between Brain Excitation and Visual Perception. *The Journal of Neuroscience*, *31*, 11889–11893.

Ergenoglu, T., Demiralp, T., Bayraktaroglu, Z., Ergen, M., Beydagi, H., & Uresin, Y. (2004). Alpha rhythm of the EEG modulates visual detection performance in humans. *Brain Research. Cognitive Brain Research*, *20*, 376–383. https://doi.org/10.1016/j.cogbrainres.2004.03.009

Fisher, R. A. (1925). Statistical methods for research workers. In S. Kotz, & N. L. Johnson (Eds.), *Breakthroughs in Statistic. Springer Series in Statistics (Perspectives in Statistics)* (pp. 66–70). Springer.

Fries, P. (2015). Rhythms for cognition: Communication through coherence. *Neuron*, *88*, 220–235. https://doi.org/10.1016/j.neuron.2015.09.034

Gallotto, S., Sack, A. T., Schuhmann, T., & de Graaf, T. A. (2017). Oscillatory correlates of visual consciousness. *Frontiers in Psychology*, *8*, 1147. https://doi.org/10.3389/fpsyg.2017.01147

Grabot, L., & Kayser, C. (2020). Alpha activity reflects the magnitude of an individual bias in human perception. *Journal of Neuroscience*, *40*, 3443–3454. https://doi.org/10.1523/JNEUROSCI.2359-19.2020

Green, D. M., & Swets, J. A. (1966). *Signal detection theory and psychophysics*. Wiley.

Gundlach, C., Moratti, S., Forschack, N., & Müller, M. M. (2020). Spatial attentional selection modulates early visual stimulus processing independently of visual alpha modulations. *Cerebral Cortex*, *30*, 3686–3703. https://doi.org/10.1093/cercor/bhz335

Iemi, L., & Busch, N. A. (2018). Moment-to-moment fluctuations in neuronal excitability bias subjective perception rather than strategic decision-making. *Eneuro*, *5*, ENEURO.0430-17.2018. https://doi.org/10.1523/ENEURO.0430-17.2018

Iemi, L., Busch, N. A., Laudini, A., Haegens, S., Samaha, J., Villringer, A., & Nikulin, V. V. (2019). Multiple mechanisms link prestimulus neural oscillations to sensory responses. *Elife*, *8*, e43620.

Iemi, L., Chaumon, M., Crouzet, S. M., & Busch, N. A. (2017). Spontaneous neural oscillations bias perception by modulating baseline excitability. *Journal of Neuroscience*, *37*, 807–819. https://doi.org/10.1523/JNEUROSCI.1432-16.2016

Keitel, C., Benwell, C. S., Thut, G., & Gross, J. (2018). No changes in parieto-occipital alpha during neural phase locking to visual quasi-periodic theta-, alpha-, and beta-band stimulation. *European Journal of Neuroscience*, *48*, 2551–2565.

Keitel, C., Keitel, A., Benwell, C. S. Y., Daube, C., Thut, G., & Gross, J. (2019). Stimulus-driven brain rhythms within the alpha band: The attentional-modulation conundrum. *Journal of Neuroscience*, *39*, 3119–3129. https://doi.org/10.1523/JNEUROSCI.1633-18.2019

Kloosterman, N. A., de Gee, J. W., Werkle-Bergner, M., Lindenberger, U., Garrett, D. D., & Fahrenfort, J. J. (2019). Humans strategically shift decision bias by flexibly adjusting sensory evidence accumulation. *Elife*, *8*, e37321. https://doi.org/10.7554/eLife.37321

Lange, J., Oostenveld, R., & Fries, P. (2013). Reduced occipital alpha power indexes enhanced excitability rather than improved visual perception. *Journal of Neuroscience*, *33*, 3212–3220. https://doi.org/10.1523/JNEUROSCI.3755-12.2013

Limbach, K., & Corballis, P. M. (2016). Prestimulus alpha power influences response criterion in a detection task: Prestimulus alpha power influences response. *Psychophysiology*, *53*, 1154–1164. https://doi.org/10.1111/psyp.12666

Macmillan, N. A., & Creelman, C. D. (2005). *Detection theory: A user's guide* (2nd ed.). Psychology Press.

Maris, E., & Oostenveld, R. (2007). Nonparametric statistical testing of EEG- and MEG-data. *Journal of Neuroscience Methods*, *164*, 177–190. https://doi.org/10.1016/j.jneumeth.2007.03.024

Mathewson, K. E., Gratton, G., Fabiani, M., Beck, D. M., & Ro, T. (2009). To see or not to see: Prestimulus phase predicts visual awareness. *Journal of Neuroscience*, *29*, 2725–2732.

Mathewson, K. E., Lleras, A., Beck, D. M., Fabiani, M., Ro, T., & Gratton, G. (2011). Pulsed Out of Awareness: EEG Alpha Oscillations Represent a Pulsed-Inhibition of Ongoing Cortical

Processing. *Frontiers in Psychology*, *2*, https://doi.org/10.3389/fpsyg.2011.00099

Milton, A., & Pleydell-Pearce, C. W. (2016). The phase of pre-stimulus alpha oscillations influences the visual perception of stimulus timing. *NeuroImage*, *133*, 53–61. https://doi.org/10.1016/j.neuroimage.2016.02.065

Oostenveld, R., Fries, P., Maris, E., & Schoffelen, J.-M. (2011). FieldTrip: Open Source Software for Advanced Analysis of MEG, EEG, and Invasive Electrophysiological Data. *Computational Intelligence and Neuroscience*, *2011*, 156869. https://doi.org/10.1155/2011/156869

Ramsøy, T. Z., & Overgaard, M. (2004). Introspection and subliminal perception. *Phenomenology and the Cognitive Sciences*, *3*, 1–23.

Romei, V., Brodbeck, V., Michel, C., Amedi, A., Pascual-Leone, A., & Thut, G. (2008). Spontaneous fluctuations in posterior alpha-band EEG activity reflect variability in excitability of human visual areas. *Cerebral Cortex*, *18*, 2010–2018.

Ronconi, L., Oosterhof, N. N., Bonmassar, C., & Melcher, D. (2017). Multiple oscillatory rhythms determine the temporal organization of perception. *PNAS*, *114*, 13435–13440. https://doi.org/10.1073/pnas.1714522114

Rouder, J. N., Speckman, P. L., Sun, D., Morey, R. D., & Iverson, G. (2009). Bayesian *t*-tests for accepting and rejecting the null hypothesis. *Psychonomic Bulletin & Review*, *16*, 225–237. https://doi.org/10.3758/PBR.16.2.225

Ruzzoli, M., Torralba, M., Morís Fernández, L., & Soto-Faraco, S. (2019). The relevance of alpha phase in human perception. *Cortex*, *120*, 249–268. https://doi.org/10.1016/j.cortex.2019.05.012

Salinas, E., & Sejnowski, T. J. (2001). Correlated neuronal activity and the flow of neural information. *Nature Reviews Neuroscience*, *2*, 539–550. https://doi.org/10.1038/35086012

Samaha, J., Bauer, P., Cimaroli, S., & Postle, B. R. (2015). Top-down control of the phase of alpha-band oscillations as a mechanism for temporal prediction. *PNAS*, *112*, 8439–8444. https://doi.org/10.1073/pnas.1503686112

Samaha, J., Gosseries, O., & Postle, B. R. (2017). Distinct oscillatory frequencies underlie Excitability of Human Occipital and Parietal Cortex. *The Journal of Neuroscience*, *37*, 2824–2833.

Samaha, J., Iemi, L., Haegens, S., & Busch, N. A. (2020). Spontaneous brain oscillations and perceptual decision-making. *Trends in Cognitive Sciences*. in press.

Samaha, J., Iemi, L., & Postle, B. R. (2017). Prestimulus alpha-band power biases visual discrimination confidence, but not accuracy. *Consciousness and Cognition*, *54*, 47–55. https://doi.org/10.1016/j.concog.2017.02.005

Samaha, J., LaRocque, J. J., & Postle, B. R. (2020). Spontaneous alpha-band amplitude predicts subjective visibility but not discrimination accuracy during high-level perception. *bioRxiv*.

Siegel, M., Donner, T. H., & Engel, A. K. (2012). Spectral fingerprints of large-scale neuronal interactions. *Nature Reviews Neuroscience*, *13*, 121–134. https://doi.org/10.1038/nrn3137

Tagliabue, C. F., Veniero, D., Benwell, C. S., Cecere, R., Savazzi, S., & Thut, G. (2019). The EEG signature of sensory evidence accumulation during decision formation closely tracks subjective perceptual experience. *Scientific Reports*, *9*, 1–12. https://doi.org/10.1038/s41598-019-41024-4

Thut, G., Miniussi, C., & Gross, J. (2012). The functional importance of rhythmic activity in the brain. *Current Biology*, *22*, 658–663.

van Diepen, R. M., Cohen, M. X., Denys, D., & Mazaheri, A. (2015). Attention and temporal expectations modulate power, not phase, of ongoing alpha oscillations. *Journal of Cognitive Neuroscience*, *27*, 1573–1586. https://doi.org/10.1162/jocn_a_00803

van Diepen, R. M., & Mazaheri, A. (2018). The caveats of observing inter-trial phase-coherence in cognitive neuroscience. *Scientific Reports*, *8*(1), 1–9. https://doi.org/10.1038/s41598-018-20423-z

VanRullen, R. (2016a). How to evaluate phase differences between trial groups in ongoing electrophysiological signals. *Frontiers in Neuroscience*, *10*, 1–22. https://doi.org/10.3389/fnins.2016.00426

VanRullen, R. (2016b). Perceptual cycles. *Trends in Cognitive Sciences*, *20*, 723–735. https://doi.org/10.1016/j.tics.2016.07.006

Varela, F., Lachaux, J. P., Rodriguez, E., & Martinerie, J. (2001). The brainweb: Phase synchronization and large-scale integration. *Nature Reviews Neuroscience*, *2*, 229–239. https://doi.org/10.1038/35067550

Vigué-Guix, I., Morís Fernández, L., Torralba Cuello, M., Ruzzoli, M., & Soto-Faraco, S. (2020). Can the occipital alpha-phase speed up visual detection through a real-time EEG-based brain-computer interface (BCI)? *European Journal of Neuroscience*.

Wöstmann, M., Waschke, L., & Obleser, J. (2019). Prestimulus neural alpha power predicts confidence in discriminating identical auditory stimuli. *European Journal of Neuroscience*, *49*, 94–105. https://doi.org/10.1111/ejn.14226

Zazio, A., Schreiber, M., Miniussi, C., & Bortoletto, M. (2020). Modelling the effects of ongoing alpha activity on visual perception: The oscillation-based probability of response. *Neuroscience and Biobehavioral Reviews*, *112*, 242–253. https://doi.org/10.1016/j.neubiorev.2020.01.037

Zhigalov, A., & Jensen, O. (2020). Alpha oscillations do not implement gain control in early visual cortex but rather gating in parieto-occipital regions. *Human Brain Mapping*, *41*, 5176–5186. https://doi.org/10.1002/hbm.25183

SUPPORTING INFORMATION

Additional Supporting Information may be found online in the Supporting Information section.